^{27}Al(p,γ)^{28}Si and ^{27}Al(^{3}He, d)^{28}Si to the stretched 11.58 MeV (6^-, 0) and 14.36 MeV (6^-, 1) levels

K. A. Snover, G. Feldman, M. M. Hindi, and E. Kuhlmann*
Department of Physics, University of Washington, Seattle, Washington 98195

M. N. Harakeh
Kernfysisch Versneller Instituut, Groningen, The Netherlands

M. Sasao and M. Noumachi
Department of Physics, Osaka University, Toyanaka, Osaka, Japan

Y. Fujita, M. Fujiwara, and K. Hosono
Research Center for Nuclear Physics, Osaka University, Suita, Osaka 565, Japan
(Received 30 September 1982)

We have studied the $E_x=14.36$ MeV $6^-,T=1$ resonance in the ^{27}Al(p,γ) reaction with the result that $\Gamma_{p_0}=\Gamma=4.0\pm0.2$ keV, from which we infer a $(d_{5/2}{}^{-1},f_{7/2})$ parentage $\delta_1{}^2\approx0.7$. We also obtain $B(M1)=2.8\pm0.4\ \mu_N{}^2$ or 0.19 ± 0.03 of the pure single particle $(d_{5/2}{}^{-1},f_{7/2})$ value for the $6^-,1\rightarrow6^-,0$ $M1$ γ decay. ^{27}Al(^{3}He, d) results for stripping to the $6^-,1$ and the $6^-,0$ (11.58 MeV) levels indicate $S_0(p)/S_1(p)=1.1\pm0.1$ and hence that the $6^-,0$ level has a $(d_{5/2}{}^{-1},f_{7/2})$ parentage comparable to the $6^-,1$ level, contrary to inferences based on inelastic proton and pion scattering data. We discuss the hindrance of the $M1$ decay and the previously measured inelastic electron, proton, and pion excitation strengths relative to the expectations of a one-particle-one-hole model.

NUCLEAR REACTIONS ^{27}Al(p,γ)^{28}Si measured $\sigma(E)$ for $J^\pi;T=6^-;1$ resonance at $E_x=14.36$ MeV. Deduced Γ, Γ_{p_0}, and Γ_γ. ^{27}Al(^{3}He,d)^{28}Si* measured $\sigma(\theta)$ for transitions to the $6^-;1$ (14.36 MeV) and $6^-;1$ (11.58 MeV) states for $E(^3\text{He})=40$ and 60 MeV. Deduced S factors from DWBA analysis and from Γ_{p_0}. Deduced $(d_{5/2}{}^{-1},f_{7/2})$ particle-hole intensity for $6^-;T$ states. Compared these results together with inelastic electron, proton, and pion scattering results with a simple particle-hole model.

I. INTRODUCTION

The "stretched" particle-hole excitations, which have the maximum possible total J for a one-particle-one-hole $1\hbar\omega$ excitation, are interesting because of their simplicity; in particular, in a $1\hbar\omega$ particle-hole model, only one configuration may contribute. States of this sort have been studied in inelastic electron and proton scattering in a number of different nuclei (see, e.g., Ref. 1) but in few cases, if any, have they been studied with several different and simple probes such that one can be reasonably sure of their nuclear structure.

In ^{28}Si, the 11.58 MeV ($6^-,T=0$) and 14.36 ($6^-,T=1$) levels have strong parentage to the stretched $(d_{5/2}{}^{-1},f_{7/2})$ configuration. They are well suited for the investigation of our understanding of inelastic electron,[2] proton,[3,4] and pion scattering[5] since they are also accessible via proton transfer, capture, and scattering. The latter reactions may be used to determine the $(d_{5/2}{}^{-1},f_{7/2})$ parentage of the 6^- levels, which can then be used to test our understanding of the inelastic scattering strengths. As we shall see, the inelastic scattering strengths are all hindered relative to strengths calculated with a simple particle-hole model based on single-nucleon spectroscopic strengths. A disadvantage of studying these negative parity levels in the middle of the *sd* shell is that there are no shell model calculations of their properties.

This paper is organized as follows: Sections II and III contain our ^{27}Al(p,γ) and ^{27}Al(^{3}He,d) measurements, respectively; Sec. IV A compares (^{3}He,d) and p_0 decay results for the $6^-,1$ level; Sec. IV B

discusses a one-particle-one-hole model and a comparison with inelastic scattering experiments; and Sec. IV C discusses the $6^-,1\rightarrow 6^-,0$ $M1$ γ-decay strengths.

II. THE ^{27}Al$(p,\gamma)^{28}$Si REACTION

The ^{27}Al$(p,\gamma)^{28}$Si reaction was studied using self-supporting Al targets, and the proton beam from the University of Washington tandem Van de Graaff. A narrow "calibration" resonance ($\Gamma=180\pm50$ eV) (Ref. 6) at $E_p=3671$ keV was studied to provide information on target thickness and beam energy spread. Results are shown in Fig. 1 for both a thick and a thin target, with the γ rays detected at $\theta_\gamma=90°$ in a large shielded NaI spectrometer. The curves shown are least-squares fits to the data of resonance yield calculations which take into account the discontinuous energy loss of the proton passing through the target. From these fits we determined that the beam energy spread (assumed Gaussian) lies in the range of 450–700 eV FWHM (full width at half maximum) and that the thick target has a thickness of 147 μg/cm^2. The thickness of the thin target (12.6 μg/cm^2) was then determined using an off-resonance thick/thin yield ratio of $(p,p_{1,2}\gamma)$ and $(p,\alpha_1\gamma)$ reaction γ rays detected in a 15% Ge(Li) detector situated at $\theta_\gamma=90°$ and a distance $D\cong5$ cm from the target.

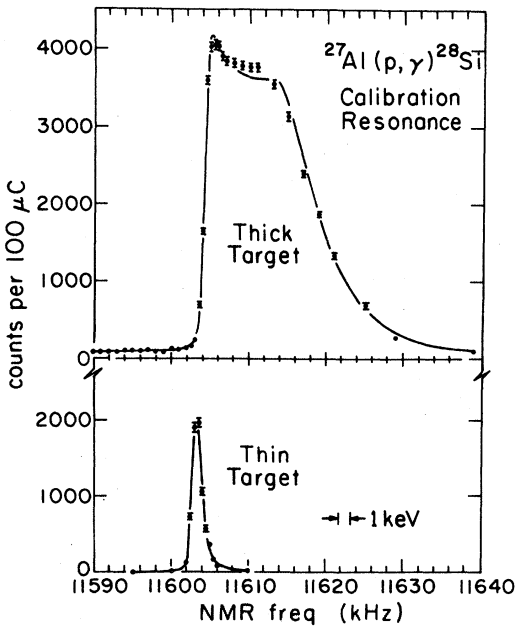

FIG. 1. Thick (147 μg/cm^2) and thin (12.6 μg/cm^2) target data over the narrow $E_p=3.671$ MeV resonance in the ^{27}Al$(p,\gamma)^{28}$Si reaction. Parameters for the calculated curves are shown in Table I.

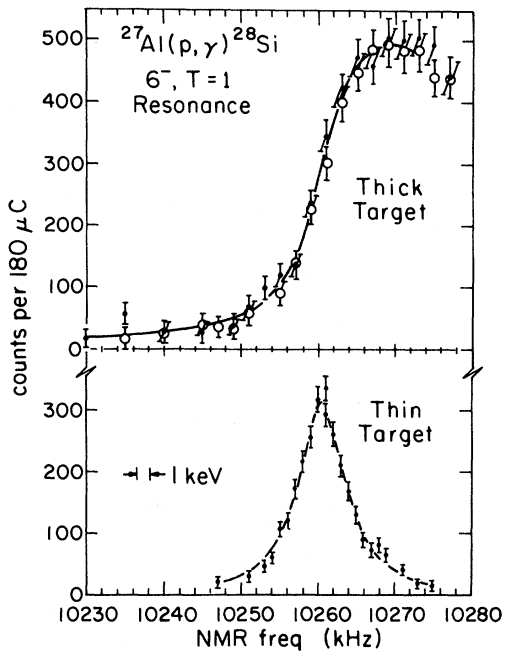

FIG. 2. Thick and thin target data over the $E_p=2876$ MeV $6^-,T=1$ resonance. Parameters for the calculated curves are shown in Table I.

Resonance yield curves were then measured for the $E_p=2876$ keV $6^-,T=1$ resonance. Shown in Fig. 2 are the resonance yields for the summed

$$(6^-,1)(14.36\text{ MeV})\rightarrow(6^-,0)(11.58\text{ MeV})$$

and

$$(6^-,0)(11.58\text{ MeV})\rightarrow(5^-,0)(9.70\text{ MeV})$$

transition intensities measured in the Ge(Li) detector. Here one clearly sees the effect of the natural resonance width on the yield. The curves shown in Fig. 2 are least-squares fits to the data of resonance yield calculations in which the resonance strength and width were varied along with a constant background, with fixed values of the energy spread and target thicknesses. Table I shows the parameters for

TABLE I. Parameters for the calculated curves shown in Figs. 1 and 2.

Resonance	Target	BES (eV)[a]	Γ (keV)[b]	t (μg/cm^2)[c]
3.671 MeV	thick	700	0.125	147
	thin	450	0.175	15
2.876	thick	800	4.10±0.53	147
	thin	450	3.78±0.19	15

[a]Beam energy spread.
[b]Center-of-mass level width.
[c]Target thickness.

TABLE II. ^{27}Al(p,γ) results for the $6^-,T=1$ resonance.

Target	Γ (keV)[b]	$\Gamma_p\Gamma_\gamma/\Gamma$ (eV)[c]
thin	3.70±0.19	0.616±0.050
thick	4.10±0.53	0.678±0.053
thin[a]	4.12±0.17	0.817±0.044
mean	4.0 ±0.2[d]	0.71 ±0.10[e]

[a]Determined in an independent measurement using a 23 μg/cm^2 target and a similar detector efficiency.
[b]Center-of-mass width.
[c]For the $6^-,1\rightarrow 6^-,0$ transition.
[d]Contains an additional ±4% estimated systematic error.
[e]Contains an additional ±8% estimated systematic error.

the calculated curves of Figs. 1 and 2. The results for the width, as shown in Table II, are insensitive to the target thickness and to changes in the beam energy spread within the range determined by the narrow resonance fits. Our average value for this width, $\Gamma=4.0\pm0.2$ keV, is in good agreement with a less precise value of 3.7±0.4 keV deduced recently from an elastic scattering experiment.[7]

In Table II, the fitted values for the resonance strength $\Gamma_p\Gamma_\gamma/\Gamma$ are listed based on our observed $6^-,1\rightarrow 6^-,0$ and $6^-,0\rightarrow 5^-,0$ intensities and on the angular distributions and branching ratios (100% for the $6^-,1\rightarrow 6^-,0$ and $6^-,0\rightarrow 5^-,0$ transitions) given in Ref. 8. The absolute detector efficiency calibration was based on measurements using calibrated ^{60}Co and ^{22}Na sources. Relative detector efficiencies were determined up to $E_\gamma=3.5$ MeV using a ^{56}Co source. The measured capture strengths $\Gamma_p\Gamma_\gamma/\Gamma$ given in Table II are for the $6^-,1\rightarrow 6^-,0$ transition, which was shown to be pure $M1$ in Refs. 8 and 9.

Previous authors reported substantially smaller capture strengths than we find for the $6^-,1\rightarrow 6^-,0$ transition. Neal and Lam[8] measured $\Gamma_p\Gamma_\gamma/\Gamma=0.32\pm0.07$ eV, while Miehe *et al.*[10] and Dalmas[11] obtained 0.23±0.08 and 0.25±0.05 eV, respectively. The reason for the discrepancy between the present result (0.71±0.10 eV) and these previous results is not clear. It may possibly be owing to the fact that the resonance has a substantial natural width and the effect of this width on the extraction of the resonance strength was not properly accounted for in previous work. Indeed, Dalmas[11] reports $\Gamma=1$ keV for this resonance. Miehe *et al.*[10] show a resonance yield curve for which substantial contributions from the tail of the resonance lie outside the energy range over which data were measured. All these authors made strength measurements relative to other ^{27}Al(p,γ) resonances whose strengths and angular distributions are, apparently, not well established.[12] These comparisons prompted us to make an independent absolute strength measurement using the same technique as we used earlier; this measurement, reported in Table II, confirms our earlier results. Hence we adopt our average strength,

$$\Gamma_p\Gamma_\gamma/\Gamma=0.71\pm0.10 \text{ eV},$$

for this decay.

In order to interpret this strength in terms of a radiative width, we must know Γ_p/Γ, the p_0 branching ratio. Since clearly $\Gamma\gg\Gamma_\gamma$, we need only know in addition the resonance strengths $\Gamma_p\Gamma_x/\Gamma$ in reaction channels $x=p_1, p_2, p_3$, and α_1 (α_0 is parity and isospin forbidden). Figure 3 shows $(p,x\gamma)$ reaction γ-ray yields in the vicinity of the $6^-,T=1$ resonance, measured with the Ge(Li) detector at $\theta_\gamma=90°$ and the thin (12.6 μg/cm^2) target. Other resonances are apparent; in p_1 a much broader resonance appears at nearly the same energy at the $6^-,1$ resonance, while p_2 and α_1 show resonances centered a few keV higher in energy. The absence of an effect in these channels due to the $6^-,1$ resonance leads to the upper limits shown in Table III. Here we in-

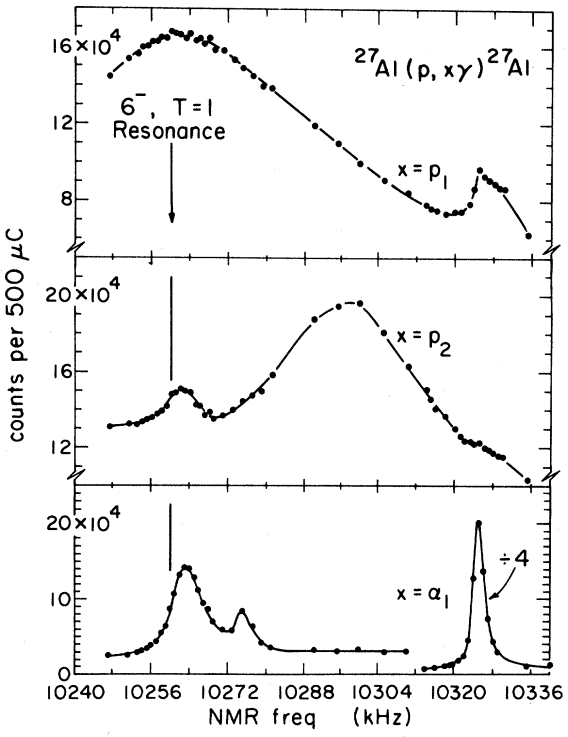

FIG. 3. Excitation energy curves for reaction γ-ray data measured in the vicinity of the $6^-,T=1$ resonance.

TABLE III. Upper limits for $6^-,T=1$ resonance strengths $\Gamma_p\Gamma_x/\Gamma$.

Channel	$\Gamma_p\Gamma_x/\Gamma$ (eV)
α_1	<12
p_1	<12
p_2	<24
p_3	<0.1
γ[a]	<0.020

[a]For the $6^-,1$ (14.36 MeV)$\rightarrow 5^-,0$ (9.70 MeV) transition.

clude results for p_3 also. Thus we conclude from our measured upper limits that $\Gamma_{p_0}/\Gamma \geq 0.99$. This result is consistent with barrier penetrability considerations, assuming equal reduced widths for all open channels. The $(d_{5/2}{}^{-1},f_{7/2})$ structure of the $6^-,1$ level would in fact favor p_0 decay. Thus to an accuracy of a few percent, $\Gamma_{p_0}/\Gamma=1.00$, and hence $\Gamma_\gamma=0.71\pm0.10$ eV.

The γ-decay strength of 0.71 ± 0.10 eV for the $6^-,1\rightarrow 6^-,0$ $M1$ transition corresponds to 1.57 ± 0.22 W.u. or $2.8\pm0.4\ \mu_N{}^2$ and hence is a relatively strong transition. Shown also in Table III is our upper limit for the "crossover"

$$(6^-,1)(14.36\text{ MeV})\rightarrow(5^-,0)(9.70\text{ MeV})$$

transition strength. This limit corresponds to

$$B(M1,6^-,1\rightarrow 5^-,0)/B(M1,6^-,1\rightarrow 6^-,0)<0.6\% .$$

Apparently this strongly hindered transition involves destructive cancellations of terms arising from different particle-hole configurations in the $5^-,0$ level.

III. THE ^{27}Al(^{3}He,d)^{28}Si REACTION

A. Experimental procedure and results

The ^{27}Al(^{3}He,d)^{28}Si reaction was studied in the region of excitation of the $6^-,T=0$ and $6^-,T=1$ states of ^{28}Si at $E_x=11.58$ and 14.36 MeV, respectively, at ^{3}He bombarding energies of 39.72 and 60.06 MeV. The ^{3}He beam obtained from the Research Center for Nuclear Physics (RCNP) cyclotron bombarded a self-supporting ^{27}Al target of 265 μg/cm^2 thickness. The deuterons corresponding to transitions in the excitation energy region of interest were detected by a position sensitive detector[13] in the focal plane of the magnetic spectrograph RAIDEN.[14] Typical energy resolution was of order 24 keV FWHM, which was more than sufficient to resolve the 6^- states from near-lying states. Some forward angle spectra were recorded with a thinner target, and $\sim$13 keV resolution. A typical energy spectrum is shown in Fig. 4.

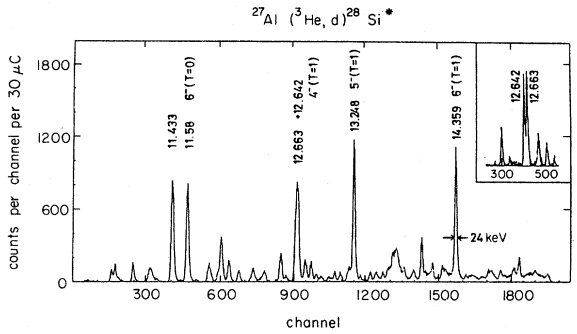

FIG. 4. Spectrum of deuterons detected in the focal plane detector of the spectrograph RAIDEN from the ^{27}Al(^{3}He,d)^{28}Si reaction at $E_{^3\mathrm{He}}=60.06$ MeV, $\theta=7°$. The inset shows the spectrum in the region of the $E_x=12.65$ MeV doublet measured with a thinner target.

Spectra were measured for angles varying from $\theta_{\mathrm{lab}}=7°$ to 65°, and $\theta_{\mathrm{lab}}=7°$ to 55° for $E_{^3\mathrm{He}}=39.72$ and 60.06 MeV, respectively. With exactly the same setup ^{3}He elastic differential cross sections were measured from $\theta_{\mathrm{lab}}=15°$ to 27° for $E_{^3\mathrm{He}}=39.72$ MeV and $\theta_{\mathrm{lab}}=12°$ to 32° for $E_{^3\mathrm{He}}=60.06$ MeV. Our elastic differential cross sections at both bombarding energies were normalized to optical model (OM) calculations; these will be further discussed in the next section. The same normalization factor was needed for both energies. The absolute cross sections determined in this manner agreed within 10% with absolute cross sections estimated using a weighted target thickness and the nominal spectrograph acceptance. As an independent check on our measured cross sections and on the angular dependence of the cross sections at small angles, we carried out limited additional measurements at $E_{^3\mathrm{He}}\approx 40.0$ MeV at Kernfysisch Versneller Instituut (KVI) Groningen using the OMG/2 magnetic spectrograph and its focal plane direction system.[15] The slightly different bombarding energy from the Osaka data is not expected to result in different cross sections. Elastic data were measured from $\theta_{\mathrm{lab}}=20°$ to 30°, and (^{3}He,d) from $\theta_{\mathrm{lab}}=0°$ to 15°. The derived absolute differential cross sections for the (^{3}He,d) reaction agreed in the overlapping region for the data from Groningen and Osaka within a few percent. The experimental and theoretical elastic differential cross sections are shown in Fig. 5.

The (^{3}He,d) reaction cross sections were normalized by the same factor used for the ^{3}He elastic cross sections. We estimate the uncertainty in the (^{3}He,d) absolute cross sections due to this normalization procedure to be less than 10%. The resulting dif-

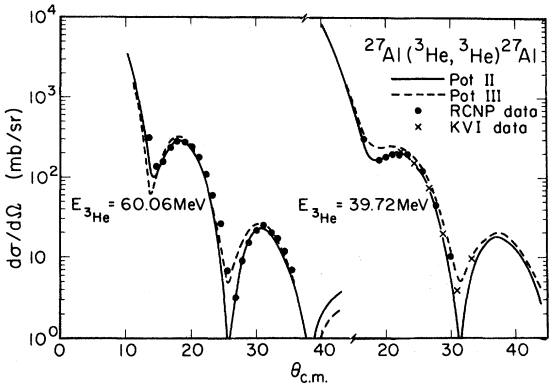

FIG. 5. Elastic scattering data for ^{3}He on ^{27}Al, $E_{^3He}=60.06$ and 39.72 MeV. The solid points are data taken at RCNP, Osaka and the crosses are data taken at KVI, Groningen. The curves correspond to optical model calculations described in the text.

ferential cross sections to the $6^-,T=0$ and $T=1$ states are shown, for both ^{3}He bombarding energies, in Fig. 6.

B. Optical model and DWBA analyses

1. Optical model calculations

OM parameters obtained for ^{3}He scattering at energies near our bombarding energies (see Table IV) were used to calculate elastic differential cross sections. The calculated results for the elastic cross sections at $E_{^3He}=39.72$ MeV are shown in Fig. 5. Better fits could be obtained to the data with Pot II (Ref. 16) which has a volume imaginary term (solid curve) than with Pot I (Ref. 17) which has a surface imaginary term (dashed curve). Our data were thus normalized to the OM calculation using parameters of Pot II.

For the data taken at $E_{^3He}=60.06$ MeV, the OM calculations using OM parameters of Pot III obtained[18] at $E_{^3He}=60$ MeV gave a reasonable fit to our data. This is shown as a dashed curve in Fig. 5. A slightly better fit (solid curve) was obtained using OM parameters of Pot II which was obtained at $E_{^3He}=37.7$ MeV. This is not surprising since the energy dependence of ^{3}He OM parameters is known[18] to be rather small in this bombarding energy region. Modifying the OM parameters of Pot II to take care of the slight energy dependence[18] of V and W affected the calculated elastic differential cross sections very little. Our elastic differential cross sections at $E_{^3He}=60.06$ MeV were normalized to the OM calculations giving more weight to the OM calculation obtained using parameters of Pot II

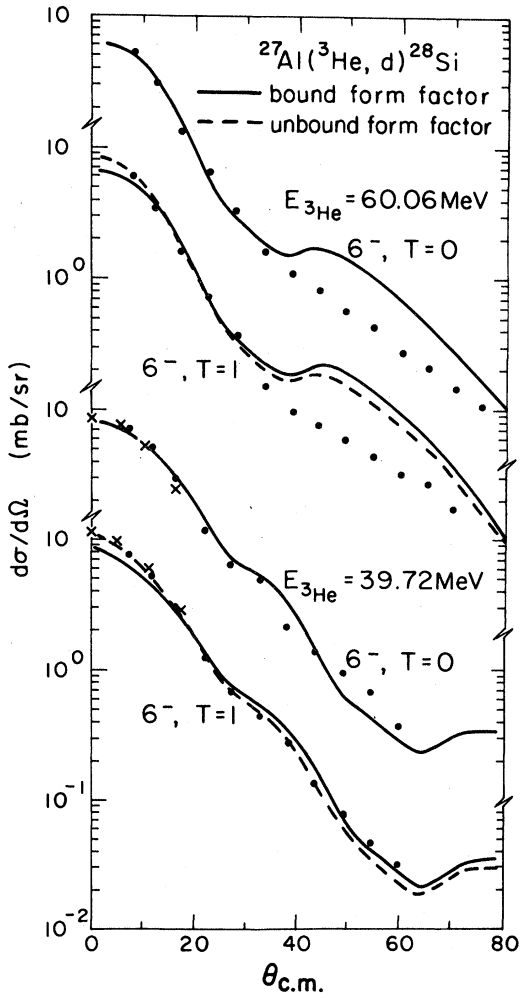

FIG. 6. ^{27}Al(^{3}He,d)^{28}Si data and DWBA calculations for the population of the $6^-,T=1$ (14.36 MeV) and $6^-,T=0$ (11.58 MeV) levels. The data points are as described in the caption of Fig. 5. The DWBA calculations are described in the text.

as shown in Fig. 5. The same normalization factor was needed to normalize the elastic differential cross sections obtained at Osaka with the same experimental setup and the same target at both bombarding energies (39.72 and 60.06 MeV) to the results of the OM calculations. This same normalization factor was used to transform the relative (^{3}He,d) cross sections into absolute cross sections.

2. DWBA analysis

The $6^-,T=0$ state at $E_x=11.58$ MeV is slightly bound (binding energy $\approx$9 keV) and hence should pose no problem for DWBA analysis. Usual DWBA calculations for stripping to bound states could be performed for this state using the energy separation method. Here the wave function of the

TABLE IV. Optical model parameters used in the DWBA calculations. The potentials are given by:

$$V(r)=V_c(r)-V_0(1+e^x)^{-1}-i\left[W_0-W'\frac{d}{dx'}\right](1+e^{x'})^{-1}+\left[\frac{\hbar}{m_\pi c}\right]^2\frac{V_{\text{s.o.}}}{r}\frac{d}{dr}(1+e^x)^{-1}(\vec{l}\cdot\vec{\sigma}),$$

where $x=(r-r_0A^{1/e})/a$ and A is the mass number of the target.

Potential	Particle	E_p[a]	V_0 (MeV)	r_R (fm)	a_R (fm)	W_0 (MeV)	W' (MeV)	r_I (fm)	a_I (fm)	$V_{\text{s.o.}}$ (MeV)	$r_{\text{s.o.}}$ (fm)	$a_{\text{s.o.}}$ (fm)	r_c (fm)	Reference
Pot I	^{3}He	41	100.7	1.185	0.734		88.0	1.342	0.706				1.40	17
Pot II	^{3}He	37.7	179.1	1.113	0.716	28.9		1.312	0.969				1.40	16
Pot III	^{3}He	60	114	1.15	0.826		75.2	1.18	0.820	2.29	1.15	0.826	1.30	18
Pot IV	d	34.4	94.3	1.056	0.814		44.04	1.353	0.733	7.0	1.056	0.814	1.30	22
Pot V	d	32.4	84.13	1.17	0.764	1.30	46.97	1.325	0.743	6.39	1.07	0.66	1.30	23
Pot VI	d	52	69.3	1.25	0.78		52.4	1.24	0.75	6.6	1.25	0.78	1.30	25
Pot VII	d	52	86.9	1.05	0.83		43.6	1.28	0.76	6.0	1.05	0.83	1.30	25
Pot VIII	d	52	79.04	1.17	0.797	3.21	41.36	1.325	0.743	5.82	1.07	0.66	1.30	23

[a]Potentials are either obtained or calculated from average parameter sets at the specified energy.

single particle is generated by a potential well whose depth is varied to fit the binding energy of the single particle. The $6^-, T=1$ state at $E_x=14.36$ MeV is, however, unbound and the single particle resonant wave function behaves asymptotically like $\sin(kr+\delta)/kr$ where δ is a phase shift; at the peak of the resonance $\delta=\pi/2$. This oscillatory behavior of the form factor outside the nucleus makes it rather difficult to get accurate DWBA cross sections using the usual integration techniques. One method that has been used quite often in the past to circumvent this problem is to slightly bind the single particle. This procedure has been shown by Vincent and Fortune[19] to lead to inaccurate results both in shape and in magnitude. Instead, a method has been developed[19] which can accurately account for the tail part of the unbound particle wave function by integrating along contours in the complex plane. In this method, a fictitious DWBA cross section $d\sigma^F/d\Omega$ is calculated. This is a function of energy; a double differential cross section is generated:

$$d^2\sigma/d\Omega\, dE=(2\mu k/\pi\hbar^2)(d\sigma^F/d\Omega)\,,$$

where μ and k are the reduced mass and wave number for the form factor channel (in our case ^{27}Al+p) which then have to be integrated over the resonance. If the resonance has a Breit-Wigner shape and is narrow and symmetric, the integration can be performed analytically and the cross section is

$$d\sigma_{\rm DWUCK}/d\Omega=(\Gamma\mu k/\hbar^2)d\sigma^F/d\Omega\,,$$

where Γ is the single particle width. Such changes have been introduced[20] into DWUCK (Ref. 21) so that the relation between the experimental cross section and the DWBA one given by DWUCK is the same as for the bound case and is given by the relation

$$d\sigma_{\rm exp}/d\Omega=NC^2S[(2J_f+1)/(2J_i+1)]\times(d\sigma_{\rm DWUCK}/d\Omega)/(2j+1)\,,$$

where $N=4.42$.

All DWBA calculations were performed using the modified version[20] of the program DWUCK.[21] To fit the (^{3}He,d) cross sections to the 6^- states obtained at $E_{^3\rm He}=39.72$ MeV, DWBA cross sections were calculated as described above. Two sets of ^{3}He OM parameters, Pot I and Pot II, and two sets of deuteron OM parameters, Pot IV (Ref. 22) and Pot V (Ref. 23), were used to check on sensitivity of DWBA cross sections to the choice of OM parameters. All four sets of DWBA calculations gave essentially equivalent fits to the experimental data.

A check on the sensitivity of the DWBA cross sections to variations in the single-particle potential parameters was also performed. These calculations were performed using a finite range correction factor of 0.77. The single-particle (s.p.) parameter sets used are listed in Table V. Pot A, B, and C represent commonly used single-particle potential parameter sets. Pot D (Ref. 24) gives the correct binding energies for orbitals near the Fermi surface and is interpolated from a local Woods-Saxon potential which fits the ^{16}O and ^{40}Ca charge radii ($\langle r^2\rangle$ and $\langle r^4\rangle$) and the values of $\langle r^2\rangle$ for the $1d_{5/2}$ and $1f_{7/2}$ neutron orbitals in ^{17}O and ^{41}Ca, respectively. Although there were little changes in the DWBA shapes for the various s.p. sets, variations in the deduced spectroscopic factors of up to 20% were observed (see Table VI). The smallest spectroscopic factors were obtained with the s.p. parameter set Pot D.

For $E_{^3\rm He}=60.06$ MeV, six sets of DWBA calculations were performed using ^{3}He OM parameter sets Pot II and Pot III and deuteron OM parameter sets Pot VI (Ref. 25), Pot VII (Ref. 25), and Pot VIII.[23]

TABLE V. Single particle potential parameters.

Potential	Particle	V_0	r	a	λ[b]	r_c
Pot A	p	a	1.2	0.65	25	1.2
Pot B	p	a	1.25	0.65	25	1.25
Pot C	p	a	1.325	0.5	25	1.325
Pot D[c]	p	a	1.296	0.651	21.6	1.366

[a]Adjusted to reproduce the binding or resonance energy.
[b]The spin-orbit term in the bound state potential is

$$+\lambda\left[\frac{\hbar}{2m_0c}\right]^2(V_0/r)\frac{d}{dr}(1+e^x)^{-1}(\vec{l}\cdot\vec{\sigma})\,,$$

where $x=(r-r_0A^{1/3})/a$ and A is the mass of the target.
[c]Reference 24 (see discussion of Sec. IV A).

TABLE VI. $f_{7/2}$ single nucleon spectroscopic factors obtained from our DWBA analysis using a finite range correction factor of 0.77 and the s.p. potential parameters given in Table V.

	$6^-, T=0$				$6^-, T=1$			
	Pot A	Pot B	Pot C	Pot D	Pot A	Pot B	Pot C	Pot D
$E_{^3\mathrm{He}}=39.72$ MeV	0.46	0.41	0.43	0.35	0.38	0.35	0.37	0.30
$E_{^3\mathrm{He}}=60.06$ MeV	0.42	0.35	0.38	0.31	0.40	0.34	0.37	0.31

Here a better fit (the backward angles shape of the DWBA cross sections was also improved compared to the experimental one) was obtained with ^{3}He OM parameter set Pot II which also gave a slightly better fit to the ^{3}He elastic cross section; all three deuteron OM parameter sets were equivalent. Again here a finite range correction factor of 0.77 was used. The results obtained using different s.p. parameter sets (see Table V) are listed in Table VI. Here again variations of up to 20% in the deduced spectroscopic factors were observed, with the smallest spectroscopic factors obtained with Pot D.

The results of the DWBA calculations using s.p. parameters set B are shown in Fig. 6. The fit to the $6^-, T=0$ state at the lower bombarding energy is good over the whole angular range. At the higher bombarding energy an equally good fit is obtained in the forward region, but for $\theta_{\mathrm{c.m.}} > 35°$ the fit deteriorates. For the $6^-, T=1$ state the DWBA calculations obtained with the unbound form factor are shown as dashed curves. DWBA calculations for this state with a bound form factor (the same binding energy as for the $T=0$ state was used) are shown as solid curves. The unbound form factor calculations give an overall better fit to the data at both bombarding energies. At the higher bombarding energy the fit to the $6^-,1$ state deteriorates for $\theta_{\mathrm{c.m.}} > 35°$, similar to the case of the $6^-,0$ state. Neither state shows a significant deviation between measured and calculated cross sections at $\theta_{\mathrm{c.m.}} < 30°$, indicating no evidence, for example, for $l=1$ transfer, which might arise if either final state were an unresolved doublet.

The single-nucleon spectroscopic factors obtained from this DWBA analysis are listed in Table VI. For both 6^- levels, the isospin Clebsch-Gordan coefficient is $C^2=0.5$, so that the tabulated single-nucleon spectroscopic factors have a maximum possible value of unity. The overall uncertainty on these spectroscopic factors is expected to be $\lesssim 20\%$ as a result of the cross section normalization and extensive DWBA analysis procedures (see, however, the discussion of Sec. IV A). From Table VI, it can be seen that the spectroscopic factors obtained at the two different bombarding energies agree to better than 20%. Moreover, it is also clear that to use a bound form factor for the $6^-, T=1$ state leads to spectroscopic factors which are about 50% higher than what is obtained with a "proper" procedure for performing DWBA calculations to unbound states.[19]

TABLE VII. Comparison of single nucleon spectroscopic factors for the $6^-, T=1$ level obtained from our (^{3}He,d) and p_0-decay analyses.

	Pot A	Pot B	Pot C	Pot D
$\Gamma_{\mathrm{s.p.}}$ (keV)	13.4	15.5	13.7	17.7
$S_1(p_0)=2\Gamma_{p_0}/\Gamma_{\mathrm{s.p.}}$[a]	0.60	0.52	0.58	0.46
$R=S_1(^3\mathrm{He},d)/S_1(p_0)$ at $E_{^3\mathrm{He}}=39.72$ MeV	0.63	0.67	0.64	0.65
$R=S_1(^3\mathrm{He},d)/S_1(p_0)$ at $E_{^3\mathrm{He}}=60.06$ MeV	0.67	0.65	0.64	0.70

[a] $\Gamma_{p_0}=4.0\pm0.2$ keV.

IV. DISCUSSION

A. Comparison of $6^-,1$ spectroscopic factors deduced from (^{3}He,d) and p_0 decay

In principle we may deduce the single nucleon spectroscopic factor $S_1(p)$ for the $6^-,1$ level from either the (^{3}He,d) analysis, as discussed in Sec. III, or from the measured p_0 decay width Γ_{p_0} through the relation

$$C^2S_1(p)=\Gamma_{p_0}/\Gamma_{\text{s.p.}} ,$$

where $C^2=0.5$ is the same isospin Clebsch-Gordan coefficient as appears in the (^{3}He,d) analysis, and $\Gamma_{\text{s.p.}}$ is the single-proton width for a pure $1f_{7/2}$ single-proton resonance at the same excitation energy. For internal consistency in this comparison, we use the same ^{27}Al+p potential well for the (^{3}He,d) analysis (Table V) as for the calculation of $\Gamma_{\text{s.p.}}$. In Table VII, the $\Gamma_{\text{s.p.}}$ values obtained from scattering in a real potential well are listed for the various s.p. potential parameters used in the DWBA analysis. Also listed are the $S_1(p_0)$, the spectroscopic factors obtained from p_0 decay according to

$$S_1(p_0)=\Gamma_{p_0}/C^2\Gamma_{\text{s.p.}} .$$

The ratios of the spectroscopic factors as obtained from the (^{3}He,d) analysis at both bombarding energies to those obtained from p_0-decay analysis for the various s.p. potential parameter sets used are listed in rows three and four. A very interesting feature emerges; namely, that

$$R=S_1(^3\text{He},d)/S_1(p_0)$$

is almost independent of the s.p. set used, although $\Gamma_{\text{s.p.}}$ varies appreciably. However, this ratio is appreciably different from the expected value of unity.

It is difficult to understand this disagreement between $S_1(^3\text{He},d)$ and $S_1(p_0)$ in terms of deficiencies in the (^{3}He,d) experiment or analysis. (See Sec. III.) In our (^{3}He,d) data, the $6^-,1$ peak sits on a small "continuum" background. If we were to ignore this background and instead ascribe all of the counts we observe under the $E_x=14.36$ MeV peak as due to the $6^-,1$ level, we would raise $S_1(^3\text{He},d)$ by 10%. In our analysis we have neglected nonlocality effects; however, the net effect of them would be to worsen the agreement between $S_1(^3\text{He},d)$ and $S_1(p_0)$ by $\sim$4%. Neglecting finite range corrections would lead to a slight worsening of the fits to the data while improving the agreement between $S_1(^3\text{He},d)$ and $S_1(p_0)$ by a factor of 1.2.

In ^{29}P a similar situation exists. The $E_x=5.739$ MeV $\frac{7}{2}^-$ state is unbound by 2.99 MeV. For this level $\Gamma_{p_0}=3.8$ keV.[12] Scattering in a real potential well calculation using Pot B (see Table V) as was used in the (^{3}He,d) analysis[26] yields $\Gamma_{\text{s.p.}}=17.4$ keV. Hence for this level S (p_0 decay) = 0.22. $S(^3\text{He},d)$ obtained from a comparison with DWBA analysis with finite range corrections is 0.12 (Ref. 27), which for this level would lead to

$$S(^3\text{He},d)/S(p_0)=0.55 .$$

Though we do not understand these discrepancies, it is clear in principle that the p_0 decay width should provide a more reliable measure of $S_1(p)$, since the (^{3}He,d) analysis has the same uncertainties as the p_0 decay analysis with regard to proton potential parameters, plus the additional uncertainty of DWBA. The problem in the p_0 decay analysis is only to determine the best value of $\Gamma_{\text{s.p.}}$. We find it difficult to choose a best value of $\Gamma_{\text{s.p.}}$ from independent considerations. Instead, we take the values given in Table VII to represent the range of possible reasonable values (13.4—17.4 keV). Halderson *et al.*[7] obtained $\Gamma_{\text{s.p.}}=10.8$ keV based on a potential derived from g-matrix considerations, a value which appears unreasonably small. Based on the results in Table VII, we adopt $\Gamma_{\text{s.p.}}=15.4\pm2$ keV. Hence

$$S_1(p_0)=2\Gamma_{p_0}/\Gamma_{\text{s.p.}}=0.52\pm0.07 .$$

From our (^{3}He,d) results, we should have a reliable estimate of $S_0(p)/S_1(p)$. From Table VI we obtain

$$S_0(p)/S_1(p)=1.1\pm0.1 .$$

This ratio is in good agreement with the value of 1.15 obtained by Nann,[28] and is significantly larger than the value of 0.93 obtained by Kato and Okada,[29] whose DWBA calculation does not provide a good fit to their $6^-,T=0$ angular distribution. Hence using $S_1(p)$ deduced from p_0 decay and our value of $S_0(p)/S_1(p)$ we obtain $S_0(p)=0.57\pm0.10$. These results are summarized with our (p,γ) results in Table VIII.

B. A one-particle-one-hole model and a comparison with inelastic scattering experiments

The 6^- levels have been studied in inelastic electron, proton, and pion scattering. Spectroscopic factors for these excitations have been deduced in the extreme $(d_{5/2}^{-1},f_{7/2})$ particle-hole model for the $6^-,T=1$ and $6^-,T=0$ levels, assuming a closed $d_{5/2}$ subshell for the ^{28}Si ground state. The results are $S_1(ee')=0.30$ (Ref. 2) to 0.33 (Ref. 4) and $S_1(p,p')=0.29$ (Refs. 3 and 4) for the $6^-,1$ level and

TABLE VIII. ^{27}Al(^{3}He,d)^{28}Si and ^{27}Al(p,γ)^{28}Si results[a] for the $6^-,T=1$ and $6^-,T=0$ levels.

Level	Reaction	$S_T(p)$[b]	Comments
$6^-,T=1$	p_0 decay	0.52±0.07	based on $\Gamma_{p_0}=4.0\pm0.2$ keV and $\Gamma_{\text{s.p.}}=15.4\pm2$ keV
$6^-,T=0$	(^{3}He,d)+p_0 decay	0.57±0.10	based on $S_0/S_1=1.1\pm0.1$ from (^{3}He,d), and $S_1(p)$ given above
$(6^-,T=1)\rightarrow(6^-,T=0)$	$M1$ γ decay		$\Gamma_\gamma=0.71\pm0.10$ eV
			$B(M1)=2.8\pm0.4\ \mu_N^2$
			$B(M1)_{\text{s.p.}}=14.4\ \mu_N^2$

[a]Present results.
[b]Single-nucleon spectroscopic factor.

$S_0(p,p')=0.10$ (Refs. 3 and 4) for the $6^-,0$ level. The 6^- states have also been observed in pion inelastic scattering, with a result for the ratio

$$S_0(\pi,\pi')/S_1(\pi,\pi')=0.4\ ,$$

(Refs. 4 and 5) similar to the value 0.34 deduced from proton inelastic scattering. We see immediately that this factor of about $\frac{1}{3}$ by which the $6^-,0$ excitation strength is reduced relative to the $6^-,1$ excitation strength in both pion and proton inelastic scattering cannot be accounted for in terms of the $(d_{5/2}{}^{-1},f_{7/2})$ parentage of the 6^- levels, since a simple one-particle-one-hole model for the 6^- levels would predict that the ratio

$$S_0(x,x')/S_1(x,x')$$

should be equal to $S_0(p)/S_1(p)$ (=1.1 from above).

In order to pursue further the quantitative relationships between the various spectroscopic strengths for proton transfer and inelastic scattering, we consider the relations between these strengths in a simple particle-hole model. We define δ_T as the $(d_{5/2}{}^{-1},f_{7/2})$ particle-hole amplitude [relative to the ^{28}Si (g.s.)] in the $6^-,T$ states, and β_1 as the $d_{5/2}{}^{-1}$ amplitude [relative to the ^{28}Si (g.s.)] in the $A=27$ (g.s). The $d_{5/2}$ nucleon pickup strength [divided by $2(2j+1)=12$] leading to the $A=27$ (g.s.) is then $\beta_1{}^2V_{5/2}{}^2$, where $V_{5/2}{}^2$ is the fractional occupancy in ^{28}Si (g.s.) of the $d_{5/2}$ orbital ($V_{5/2}{}^2=1$ for a filled $d_{5/2}$ orbital). Thus $V_{5/2}{}^2$ is the total nucleon pickup strength (divided by 12) to all $\frac{5}{2}^+$ states in mass 27. The "other" configurations of intensity $1-\delta_T{}^2$ in the $6^-,1$ states and $1-\beta_1{}^2$ in the $A=27$ (g.s.) lie outside our particle-hole basis and are assumed not to contribute to the matrix elements of interest. With this assumption we obtain

$$\delta_T{}^2=S_T(p)/\beta_1{}^2=S_T(x,x')/V_{5/2}{}^2\ ,$$

where $S_T(p)$ is the single nucleon spectroscopic factor, and $S_T(x,x')$ is the direct one-step inelastic scattering spectroscopic amplitude deduced assuming a filled $d_{5/2}$ orbital in the ^{28}Si (g.s.).

We estimate $V_{5/2}{}^2$ from the summed nucleon pickup strength to $\frac{5}{2}^+$ states in mass 27;

$$V_{5/2}{}^2=(6.4+1.2+0.6)/12=0.68\ ,$$

(see Refs. 12 and 30). Here we have included pickup strength to the three lowest $\frac{5}{2}^+$ states. In order to make sure that we are not omitting significant unobserved pickup strength to higher $\frac{5}{2}^+$ states in mass 27, we look at single-nucleon stripping on ^{28}Si to $\frac{5}{2}^+$ states in mass-29; we find a total $d_{5/2}$ stripping strength of $0.19+0.10=0.29$ to the two lowest $\frac{5}{2}^+$ states.[30] Thus the total $d_{5/2}$ (pickup + stripping) strength on ^{28}Si is $0.68+0.29=0.97$, close to the value of unity expected in the absence of significant unobserved strength. Alternatively, we may check the total pickup strength to positive parity states in mass 27. For states below $E_x=5$ MeV, the result is[30] $11.1+0.6=11.7$, which is quite close to the expected value of 12. Chung and Wildenthal[31] calculate $V_{5/2}{}^2=0.76$ for ^{28}Si, in reasonable agreement with the experimental estimate of 0.68. The factor $\beta_1{}^2$, the fractional amount of $d_{5/2}$ pickup strength to mass 27 which goes to the ground state, is experimentally from above,

$$\beta_1{}^2\cong6.4/8.2=0.78\ .$$

The results of this analysis are shown in Table IX. One immediately sees that our estimates of $\delta_T{}^2$, the $(d_{5/2}{}^1,f_{7/2})$ intensity in the $6^-,T$ levels, based on $S_T(p)$ and $S_T(x,x')$ for $x=e$ or p, are not in good agreement. Our estimates of $\delta_T{}^2$ based on $S_T(p)$ should be most reliable, since they are least likely to be affected by deficiencies of our simple particle-

TABLE IX. $(d_{5/2}{}^{-1},f_{7/2})$ intensities $\delta_T{}^2$ for the $6^-,T$ levels and a comparison with inelastic scattering results.[a]

Level	Reaction	$\delta_T{}^2=S_T(p)/\beta_I{}^2$	$S_T(x,x')/V_{5/2}{}^2$
$6^-,T=1$	p_0 decay	0.67±0.09	
	(e,e')[c]		$\frac{0.30-0.33}{0.68}=0.44-0.49$
	(p,p')[d]		$\frac{0.29}{0.68}=0.43$
$6^-,T=0$	p_0 decay $(6^-,1)$[b] + $(^3$He,$d)$ ratio	0.73±0.12	
	(p,p')[d]		$\frac{0.10}{0.68}=0.15$
$6^-,T=0/6^-,T=1$	$(^3$He,$d)$ ratio[b] $S_0/S_1=1.1$		
	(p,p') ratio[d]	0.34	
	(π,π') ratio[e]	0.40	
$6^-,1\rightarrow 6^-,0$ $M1$ decay[b]		$B(M1)/B(M1)_{s.p.}=0.19\pm0.03$ (expt.) $=\approx 0.3$ (calc.)	

[a]Assuming $\beta_1{}^2=0.78$ and $V_{5/2}{}^2=0.68$ (see text).
[b]Present work.
[c]References 2 and 4.
[d]References 3 and 4.
[e]Reference 5.

hole model. Hence we adopt the $(d_{5/2}{}^{-1},f_{7/2})$ intensities $\delta_1{}^2=0.67\pm0.09$ for the $6^-,1$ level and $\delta_0{}^2=0.73\pm0.12$ for the $6^-,0$ level.

In contrast to this analysis, the authors of Ref. 7 argued on the basis of a similar model that $S_1(p)$ and $S_1(e,e')$ are compatible. Our conclusions differ primarily for two reasons: they failed to account for the fractionation of $d_{5/2}$ pickup strength (i.e., they assumed $\beta_1{}^2=1.0$), and they used an older and smaller value for the

$$^{28}\text{Si (g.s.)}\rightarrow A=27\text{ (g.s.)}$$

pickup strength of 0.44(12) compared to our value[30] of

$$0.78(0.68)(12)=0.53(12)\ .$$

The inelastic scattering experiments excite the 6^- levels more weakly than expected (Table IX). For electron scattering to the $6^-,1$ level, the $M6$ reduction (relative to our 1p-1h expectation) is

$$S_1(e,e')/\delta_1{}^2V_{5/2}{}^2\approx 0.7\ .$$

This is due presumably to the combined effects of mesonic exchange currents are core polarization. Ejiri and Fujita[32] found hindered matrix elements $(g^{\text{eff}}/g\sim 0.2-0.5)$ for a variety of $L=1-4$ spin, spin-isospin and isospin γ, and β transitions in medium and heavy nuclei, interpreted as primarily due to effects of core polarization. The observed $M6$ hindrance corresponds to

$$g^{\text{eff}}/g\sim\sqrt{0.7}=0.85\ .$$

It seems reasonable that core polarization effects on "low-lying" transitions should decrease with increasing multipolarity L since the "giant resonance" energy should increase with L (for our $M6$, the unperturbed "giant" strength is approximately 30% $3\hbar\omega$ and 60% $5\hbar\omega$).[33] On the other hand, mesonic exchange currents are expected to enhance the transition strength at large momentum transfer, which would increase g^{eff}/g. It is interesting to note that a similar hindrance[34] is found for $M12$ and $M14$ excitations in ^{208}Pb, interpreted by Krewald and Speth[35] as being due primarily to the fragmentation of 1p-1h strength in the excited state. A similar hindrance has been found for a variety of lower multipolarity ML and transverse EL excitations[36] in ^{207}Pb.

The $6^-,1$ excitation is hindered to a similar degree in electron and proton scattering, while both proton and pion scattering excite the $6^-,0$ level anomalously weakly (Table IX). [See also the recent (p,p') analysis of Ref. 37 which gives $S_0(p,p')\sim 0.15$.] We argued above that the relative weakness of the $6^-,0$ excitation cannot be explained in terms of differing $(d_{5/2}{}^{-1},f_{7/2})$ parentage in the $6^-,T$ level, based on the proton transfer results. It is also unlikely to be explainable in terms of core polarization differences. To the degree that the nuclear exchange interaction is predominantly of a Majorana type, the isoscalar and isovector $M6$ excitation should experience similar hindrances due to

core polarization.[32] Perhaps there is a problem in the extraction of $S_0(x,x')$ or

$$S_0(x,x')/S_1(x,x')$$

from the measured pion and proton inelastic scattering cross sections. The assumed isoscalar spin-spin projectile nucleon interaction may be much weaker than previously believed.

C. The $6^-,1\rightarrow 6^-,0$ $M1$ γ-decay strength

The observed $6^-,1\rightarrow 6^-,0$ $M1$ decay strength of 0.70 ± 0.10 eV corresponds to $B(M1)=2.8\pm0.4$ $\mu_N{}^2$. The calculated "single particle" strength for pure $(d_{5/2}{}^{-1},f_{7/2})6^-,T$ configurations assuming nucleon g factors is $B(M1)_{\text{s.p.}}=14.4\,\mu_N{}^2$; hence,

$$B(M1)/B(M1)_{\text{s.p.}}=0.19\pm0.03\ .$$

Thus this rather strong $M1$ transition is significantly inhibited relative to the single particle estimate. The latter may be obtained from

$$B(M1)=|\,1.77\mu_{5/2}/\mu_{5/2,S}+2.03\mu_{7/2}/\mu_{7/2,S}\,|^2\ ,$$

where $\mu_{5/2}$ and $\mu_{7/2}$ are the isovector $d_{5/2}$ and $f_{7/2}$ magnetic moments, and $\mu^{\text{IV}}=(\mu_p-\mu_n)$. The quantities $\mu_{5/2,S}=6.71$ and $\mu_{7/2,S}=7.71$ are the Schmidt isovector single nucleon $d_{5/2}$ and $f_{7/2}$ magnetic moments in units of μ_N. $B(M1)_{\text{s.p.}}$ is obtained from the above equation with the $d_{5/2}$ and $f_{7/2}$ magnetic moments set equal to their Schmidt values. Thus $B(M1)_{\text{s.p.}}$ is large because it is a coherent sum of terms proportional to the (large) $d_{5/2}$ and $f_{7/2}$ magnetic moments.

Within the framework of our simple one-particle one-hole model discussed in Sec. IV B, we would expect

$$B(M1)/B(M1)_{\text{s.p.}}=\delta_1{}^2\cdot\delta_0{}^2=0.49\pm0.14\ .$$

A substantial part of the difference between this estimate and the measured strength is expected to be due to $0\hbar\omega$ $M1$ core polarization. Such polarization effects are known to reduce the magnitude of ground-state magnetic moments.[38] In our model, we would expect

$$\mu_{5/2}(A=27\text{ g.s.})/\mu_{5/2,S}=\beta_1{}^2=0.78\ ,$$

whereas the experimental value is 0.67.[39,40] Hence we may crudely estimate the further reduction due to $0\hbar\omega$ $M1$ core polarization as

$$\delta\mu_{5/2}/\mu_{5/2,S}=0.67/0.78=0.86\ .$$

Large basis shell model calculations in the *sd* shell show that no further reduction of $\mu(d_{5/2})$ is necessary[41] (such as might be due to mesonic exchange or many $\hbar\omega$ core polarization). However,

$$\mu_{7/2}(A=41\text{ g.s.})/\mu_{7/2,S}=0.9$$

(Ref. 39) apparently represents such an effect.[42] Thus we estimate

$$\delta\mu_{7/2}/\mu_{7/2,S}=0.9(0.86)=0.77$$

near $A=28$. This leads to a calculated value of

$$B(M1)/B(M1)_{\text{s.p.}}=0.66\delta_1{}^2\cdot\delta_0{}^2=0.3\ ,$$

in reasonable agreement with the experimental ratio.

ACKNOWLEDGMENTS

One of us (K.A.S.) would like to thank the Japan Society for the Promotion of Science for fellowship support during part of this work, Prof. H. Ejiri for valuable discussions, and Prof. H. Ikegami and the staff of the Research Center for Nuclear Physics for their hospitality.

---

*Present address: Ruhr-Universität Bochum D-4630 Bochum-Querenberg, Federal Republic of Germany.

[1]R. A. Lindgren, W. J. Gerace, A. D. Bacher, W. G. Love, and F. Petrovich, Phys. Rev. Lett. 42, 1524 (1979).

[2]S. Yen, R. Sobie, H. Zarek, B. O. Pich, T. E. Drake, C. F. Williamson, S. Kowalski, and C. P. Sargent, Phys. Lett. 93B, 250 (1980).

[3]G. S. Adams, A. D. Bacher, G. T. Emery, W. P. Jones, R. T. Kouzes, D. W. Miller, A. Picklesimer, and G. E. Walker, Phys. Rev. Lett. 38, 1387 (1977).

[4]F. Petrovich, W. G. Love, A. Picklesimer, G. E. Walker, and E. R. Siciliano, Phys. Lett. 95B, 166 (1980).

[5]C. Olmer, B. Zeidman, D. F. Geesaman, T.-S. H. Lee, R. E. Segel, L. W. Swenson, R. L. Boudrie, G. S. Blanpied, H. A. Thiessen, C. L. Morris, and R. E. Anderson, Phys. Rev. Lett. 43, 612 (1979).

[6]J. L. Osborne, E. G. Adelberger, and K. A. Snover, Nucl. Phys. A305, 144 (1978).

[7]D. Halderson, K. W. Kemper, J. D. Fox, R. O. Nelson, E. G. Bilpuch, C. R. Westerfeldt, and G. E. Mitchell, Phys. Rev. C 24, 786 (1981).

[8]G. F. Neal and S. T. Lam, Phys. Lett. 45B, 127 (1973).

[9]G. F. Neal and P. R. Chagnon, Phys. Rev. C 11, 1461 (1975).

[10]C. Miehe, J. P. Gonidec, A. Huck, and G. Walter, Rev.

Phys. Appl. 8, 307 (1973).
[11]M. J. Dalmas, C. R. Acad. Sci. Paris 277B, 237 (1973).
[12]P. M. Endt and C. van der Leun, Nucl. Phys. A310, 1 (1978).
[13]Y. Fujita, K. Nagayama, S. Morinobu, M. Fujiwara, I. Katayama, T. Yamazaki, and H. Ikegami, Nucl. Instrum. Methods 173, 265 (1980).
[14]H. Ikegami, S. Morinobu, I. Katayama, M. Fujiwara, and S. Yamabe, Nucl. Instrum. Methods 175, 335 (1980).
[15]A. G. Drentje, H. A. Enge, and S. B. Kowalski, Nucl. Instrum. Methods 122, 485 (1974); J. C. Vermeulen, J. van der Plicht, A. G. Drentje, L. W. Put, and J. van Driel, *ibid.* 180, 93 (1981).
[16]C. M. Perey and F. C. Perey, Nucl. Data Tables 17, 1 (1976).
[17]H.-J. Trost *et al.*, Nucl. Phys. A337, 377 (1980).
[18]E. F. Gibson, B. W. Ridley, J. J. Kraushaar, M. E. Rickey, and R. H. Bassel, Phys. Rev. 155, 1194 (1967).
[19]C. Vincent and H. T. Fortune, Phys. Rev. C 2, 782 (1970).
[20]J. R. Comfort, private communication.
[21]P. D. Kunz, DWUCK program, University of Colorado (unpublished).
[22]E. Newman, L. C. Becker, and B. M. Preedom, Nucl. Phys. A100, 225 (1967).
[23]W. W. Daehnick, J. D. Childs, and Z. Vrcelj, Phys. Rev. C 21, 2253 (1980).
[24]B. A. Brown, private communication.
[25]F. Hinterberger, G. Mairle, U. Schmidt-Rohr, G. J. Wagner, and P. Turek, Nucl. Phys. A111, 265 (1968).
[26]W. W. Dykoski and D. Dehnhard, Phys. Rev. C 13, 80 (1976).
[27]The spectroscopic factors quoted here are from a reanalysis performed by us assuming an $f_{7/2}$ transfer consistent with the assignment of $\frac{7}{2}^-$ to this level by Endt and van der Leun (Ref. 12), as opposed to $f_{5/2}$ transfer assumed by Dykoski and Dehnhard (Ref. 26). In the reanalysis we used the optical model and single particle parameters of Ref. 26.
[28]H. Nann, Nucl. Phys. A376, 61 (1982).
[29]S. Kato and K. Okada, J. Phys. Soc. Jpn. 50, 1440 (1981).
[30]P. M. Endt, At. Data Nucl. Data Tables 19, 49 (1977).
[31]W. Chung, Ph.D thesis, Michigan State University, 1976 (unpublished); B. H. Wildenthal, in *Elementary Modes of Excitation in Nuclei,* edited by R. Broglia and A. Bohr (North-Holland, Amsterdam, 1977), p. 383; and private communication.
[32]H. Ejiri and J. I. Fujita, Phys. Rep. 38, 87 (1978), and references therein.
[33]G. E. Walker, private communication.
[34]J. Lichtenstadt, J. Heisenberg, C. N. Papanicolas, C. P. Sargent, A. N. Courtemanche, and J. S. McCarthy, Phys. Rev. Lett. 40, 1127 (1978); Phys. Rev. C 20, 497 (1979).
[35]S. Krewald and J. Speth, Phys. Rev. Lett. 45, 417 (1980).
[36]C. N. Papanicolas, J. Lichtenstadt, C. P. Sargent, J. Heisenberg, and J. S. McCarthy, Phys. Rev. Lett. 45, 106 (1980).
[37]G. T. Emery, A. D. Bacher, and C. Olmer, Proceedings of the International Conference on Spin Excitation in Nuclei, Telluride, Colorado, 1982 (Plenum, New York, to be published).
[38]A. Arima and H. Horie, Prog. Theor. Phys. 11, 509 (1954); 12, 623 (1954).
[39]*Tables of Isotopes,* 7th edition, edited by C. M. Lederer and V. S. Shirley (Wiley, New York, 1978).
[40]J. W. Hugg and S. S. Hanna, *Proceedings of the International Conference on Nuclear Physics, Berkeley, California 1980,* edited by R. M. Diamond and J. O. Rasmussen (North-Holland, Amsterdam, 1981), p. 104.
[41]B. A. Brown, W. Chung, and B. H. Wildenthal, Phys. Rev. C 22, 774 (1980).
[42]J. B. McGrory and B. H. Wildenthal, Phys. Lett. 103B, 173 (1981).